J. Fluid Mech. (1986), *vol.* 165, *pp.* 425–444
Printed in Great Britain

Vertical drift and reaction effects upon contaminant dispersion in parallel shear flows

By RONALD SMITH

Department of Applied Mathematics and Theoretical Physics, University of Cambridge, Silver Street, Cambridge CB3 9EW

(Received 18 June 1985 and in revised form 17 October 1985)

It is shown how the effects of the initial discharge profile, vertical drift, and boundary absorption (catalytic reaction) can be incorporated into a Gaussian approximation for the two-dimensional contaminant distribution in a parallel shear flow. Exact and asymptotic expressions are derived for the centroid displacement, shear-dispersion coefficient, and variance. Detailed results are presented for the effect of absorption at the bed and of vertical drift velocities upon contaminant dispersion in turbulent open-channel flow. For both cases the advantages of discharges close to the bed over surface discharges are made quantitative.

1. Introduction

Contaminant dispersion in a shear flow is an intrinsically multi-dimensional process. Material in different parts of the flow is carried along at the local flow velocity. Thus, soon after discharge there can be considerable shear distortions of the concentration distribution (Sullivan 1971, figure 1; Fischer *et al.* 1979, figure 5.15). In chemical-engineering processes this distortion by the longitudinal flow can be further complicated by a species-dependent vertical drift velocity, or by absorption (catalytic reaction) at the wall. Illustrations of the extent to which a vertical drift can change the magnitude and distribution of concentration are given by Jayaraj & Subramanian (1978, figures 2 and 7, 6 and 9).

Mathematical models for shear-flow dispersion are usually formulated in terms of some weighted average of the concentration profile across the flow (Sankarasubramanian & Gill 1973; Krishnamurthy & Subramanian 1977; Hsieh, Lee & Gill 1979; Lungu & Moffatt 1982; Smith 1983*a*, *b*). Such one-dimensional model equations have a formal range of validity restricted to large times after discharge, when the concentration profile across the flow has equilibrated. At moderate times after discharge the results can be seriously in error (Jayaraj & Subramanian 1978, figures 3, 4, 12, 13; Smith 1983*a*, figure 6; Smith 1983*b*, figure 10).

The author (Smith 1982) has given a Gaussian description for the two-dimensional contaminant distribution in a shear flow. Unlike the one-dimensional models, it is particularly efficient at moderate times after discharge. However, it was only applied to uniform discharges with zero drift and impermeable boundaries. The purpose of the present paper is to extend the model to include all three complications, i.e. arbitrary discharge profiles, vertical drift, and boundary absorption (catalytic reaction). At each level across the flow the contaminant distribution associated with any elementary discharge $q(\hat{y})\,\mathrm{d}\hat{y}$ is modelled as being Gaussian. Equations are derived for the integrated concentration, centroid, and variance within each level. Closely related work, focusing attention on the large-time behaviour, has been presented by Barton (1984).

There has been much public debate in the UK concerning accidental discharges of high-level radioactive waste into the Irish sea from storage tanks at the Sellafield nuclear reprocessing plant. A distinctive feature of transuranic elements is their affinity for bottom sediments. The first detailed example studied in this paper investigates this effect. As we might expect, the take-up of contaminants into the sediments is more rapid when the effective discharge height is close to the bed. The second illustrative example concerns the effect of vertical drift velocities. Since the shear is greatest near the bed, the dilution tends to be more rapid for sinking contaminants. Also, to take immediate advantage of the shear and enhanced dilution, it is preferable for discharges to be at the bed rather than near the surface.

2. Gaussian approximation

The equation that we shall seek to solve is the two-dimensional advection–diffusion equation

$$\partial_t c + \alpha c + u\partial_x c + \partial_y(vc) = \kappa_L \partial_x^2 c + \partial_y(\kappa \partial_y c), \tag{2.1a}$$

with the boundary conditions

$$vc - \kappa \partial_y c = \beta_+ c \quad \text{on} \quad y = y_+, \tag{2.1b}$$

$$vc - \kappa \partial_y c = -\beta_- c \quad \text{on} \quad y = y_-, \tag{2.1c}$$

and the initial discharge distribution

$$c = q(y)\,\delta(x) \quad \text{at} \quad t = 0. \tag{2.1d}$$

Here α is the reaction rate in the body of the fluid, $u(y)$ the primary longitudinal flow, v the vertical drift, κ_L the longitudinal diffusivity, $\kappa(y)$ the vertical diffusivity, β_+, β_- the reaction (absorption) coefficients at the boundaries, and y_+, y_- are the boundary positions. If the vertical drift is a property of the main flow, then by mass conservation v must be constant. However, if there is a species-dependent drift relative to the main flow caused by some external force field, then v can be a function of y.

Rather than solving (2.1*a–d*) numerically, as done by Jayaraj & Subramanian (1978), we shall follow Smith (1982) and Barton (1984) by seeking a Gaussian approximation

$$c = \int_{y_-}^{y_+} \mathrm{d}\hat{y}\, \frac{q(\hat{y})}{(2\pi)^{\frac{1}{2}}\sigma} \exp\left(-\tfrac{1}{2}\xi^2\right) a^{(0)}(y, t; \hat{y}), \tag{2.2a}$$

with

$$\xi = \frac{x - X}{\sigma}. \tag{2.2b}$$

Here $X(y, t; \hat{y})$ and $\sigma^2(y, t; \hat{y})$ respectively are the centroid displacement and variance at the level y across the flow associated with an elementary discharge at the level $\hat{y}$.

For an unbounded linear shear, with constant diffusivities, this Gaussian representation is exact (Townsend 1951). However, in general (2.2*a*) must be regarded as being the first term in a series expansion, as explained in Appendix A. The equations satisfied by the coefficients $a^{(0)}$, X, σ^2 can be derived by taking the zero, first and second moments with respect to x of (2.1*a–d*). Hence any errors are relegated to the third and higher moments. This derivation is systematized and extended in Appendix A.

A generalization to three dimensions can be achieved by allowing $a^{(0)}$ to be a function of z, $\hat{z}$. More simply, if the problem is uniform and unbounded with respect to z, an additional Gaussian factor can be included in the representation (2.2a):

$$\exp(-\tfrac{1}{2}\zeta^2)/(2\pi)^{\frac{1}{2}}\sigma_3, \tag{2.3a}$$

with

$$\zeta = \frac{z-\hat{z}}{\sigma_3}. \tag{2.3b}$$

The absence of crossflow makes the z-structure much more simple than the x-structure. For example, the centroid has the constant value $\hat{z}$.

It is possible to adapt the calculations to apply to even more complicated situations. For example, Doshi, Gill & Subramanian (1975) show that by a change of variables

$$u^* = u\left(1-\frac{x^*}{L}\right), \quad \frac{x^*}{L} = 1-\exp\left(-\frac{x}{L}\right), \tag{2.4}$$

(2.1a–d) also apply to the industrially relevant case in which the vertical drift is achieved by uniform suction through the boundary in a channel of length L.

3. Eigenfunction expansions

The Gaussian representation (2.2a) deals with the longitudinal structure of the solution. However, there still remains the task of calculating the y, t structure. The starting point is the equation satisfied by the amplitude factor $a^{(0)}(y, t; \hat{y})$:

$$\partial_t a^{(0)} + \alpha a^{(0)} + \partial_y(v a^{(0)}) - \partial_y(\kappa\, \partial_y a^{(0)}) = 0, \tag{3.1a}$$

with

$$(v-\beta_+)\, a^{(0)} - \kappa\, \partial_y a^{(0)} = 0 \quad \text{on} \quad y = y_+, \tag{3.1b}$$

$$(v+\beta_-)\, a^{(0)} - \kappa\, \partial_y a^{(0)} = 0 \quad \text{on} \quad y = y_-, \tag{3.1c}$$

and

$$a^{(0)} = \delta(y-\hat{y}) \quad \text{at} \quad t = 0 \tag{3.1d}$$

(see Appendix A equation (A 1) with $m = 0$). In this section we will derive solutions for small, moderate and large times after discharge.

At small times the boundary can be regarded as being remote, and the velocity shear as being locally linear. Thus, the exact solution derived by Townsend (1951) provides the basis for an asymptotic solution. The distorted Gaussian solution for $a^{(0)}$ is

$$a^{(0)} = \frac{1}{(4\pi t)^{\frac{1}{2}}[\kappa(y)\,\kappa(\hat{y})]^{\frac{1}{4}}} \exp\left(-\frac{\rho^2}{4t}\right), \tag{3.2a}$$

with

$$\rho^2 = \left[\int_{\hat{y}}^{y} \frac{\mathrm{d}y'}{\kappa^{\frac{1}{2}}}\right]^2 - \frac{2}{t}\int_{\hat{y}}^{y} \frac{v}{\kappa}\,\mathrm{d}y' + \ldots. \tag{3.2b}$$

The second term in (3.2b) has the obvious interpretation that for small times the contaminant moves upwards with the drift velocity v.

We remark that in the absence of depletion, either in the body of the fluid ($\alpha = 0$) or at the boundaries ($\beta = 0$), the equilibrium solution for the concentration profile across the flow is

$$\gamma(y) = \exp\left[\int_{y_*}^{y} \frac{v}{\kappa}\,\mathrm{d}y'\right]. \tag{3.3}$$

A convenient choice for the reference level y_* is to ensure that

$$\overline{\gamma^{\frac{1}{2}}\psi_0} = 1, \tag{3.4}$$

where the equilibrium eigenmode $\psi_0(y)$ is defined in (3.8) below, and the overbar denotes the cross-sectional average value.

To solve (3.1*a–d*) we first factor-out $\gamma^{\frac{1}{2}}$:

$$a^{(0)}(y, t; \hat{y}) = \gamma^{\frac{1}{2}}(y)\, b^{(0)}(y, t; \hat{y}). \tag{3.5}$$

This factorization removes any counterpart to $\partial_y(va^{(0)})$ in the field equation for $b^{(0)}$:

$$\partial_t b^{(0)} + \left[\alpha + \tfrac{1}{2}\partial_y v + \frac{1}{4}\frac{v^2}{\kappa}\right] b^{(0)} - \partial_y(\kappa\, \partial_y b^{(0)}) = 0, \tag{3.6a}$$

with

$$(\tfrac{1}{2}v - \beta_+)\, b^{(0)} - \kappa\, \partial_y b^{(0)} = 0 \quad \text{on} \quad y = y_+, \tag{3.6b}$$

$$(\tfrac{1}{2}v + \beta_-) - \kappa\, \partial_y b^{(0)} = 0 \quad \text{on} \quad y = y_-, \tag{3.6c}$$

and

$$b^{(0)} = \delta(y - \hat{y})\, \gamma^{-\frac{1}{2}}(\hat{y}) \quad \text{at} \quad t = 0. \tag{3.6d}$$

The separation-of-variables solution for $b^{(0)}$ can be written

$$b^{(0)} = \gamma^{-\frac{1}{2}}(\hat{y}) \sum_{m=0}^{\infty} \psi_m(\hat{y})\, \psi_m(y) \exp(-\lambda_m t), \tag{3.7}$$

where the eigenfunctions $\psi_m(y)$ and eigenvalues λ_m satisfy the Sturm–Liouville equations

$$\frac{\mathrm{d}}{\mathrm{d}y}\left[\kappa \frac{\mathrm{d}}{\mathrm{d}y}\psi_m\right] + \left[\lambda_m - \alpha - \tfrac{1}{2}\partial_y v - \frac{1}{4}\frac{v^2}{\kappa}\right]\psi_m = 0, \tag{3.8a}$$

with

$$[\tfrac{1}{2}v - \beta_+]\,\psi_m - \kappa\, \partial_y \psi_m = 0 \quad \text{on} \quad y = y_+, \tag{3.8b}$$

$$[\tfrac{1}{2}v + \beta_-]\,\psi_m - \kappa\, \partial_y \psi_m = 0 \quad \text{on} \quad y = y_-, \tag{3.8c}$$

and

$$\overline{\psi_m^2} = 1, \quad \overline{\psi_m \psi_n} = 0 \quad \text{for} \quad m \neq n. \tag{3.8d, e}$$

In the absence of depletion mechanisms ($\alpha = 0$, $\beta = 0$) the lowest mode is given by

$$\psi_0 = \gamma^{\frac{1}{2}}, \quad \text{with} \quad \lambda_0 = 0 \tag{3.9}$$

(Krishnamurthy & Subramanian 1977, equation A 12). For α or β positive the lowest eigenvalue λ_0 is positive.

The corresponding series expansion for $a^{(0)}(y, t; \hat{y})$ is

$$a^{(0)} = \gamma^{-\frac{1}{2}}(\hat{y})\, \gamma^{\frac{1}{2}}(y) \sum_{m=0}^{\infty} \psi_m(\hat{y})\, \psi_m(y) \exp(-\lambda_m t) \tag{3.10}$$

(Barton 1984, equation 2.5). Hence, the concentration profile across the flow equilibrates to

$$a^{(0)} \doteq \gamma^{-\frac{1}{2}}(\hat{y})\, \gamma^{\frac{1}{2}}(y)\, \psi_0(\hat{y})\, \psi_0(y) \exp(-\lambda_0 t) \tag{3.11}$$

on the timescale $1/(\lambda_1 - \lambda_0)$. A noteworthy feature is that when there is depletion there is a persistent dependence upon the discharge level $\hat{y}$. This is why, in a paper directed towards the large-time behaviour, Barton (1984, §2) gives attention to the early

development. The normalization (3.4) means that the fractional amount of contaminant remaining in the fluid asymptotes to

$$\gamma^{-\frac{1}{2}}(\hat{y})\,\psi_0(\hat{y})\,\exp(-\lambda_0 t). \tag{3.12}$$

Neat results such as this are an important justification for analytic as opposed to computational studies of contaminant dispersion.

Fischer *et al.* (1979, §5.5) warn that for one-dimensional (equilibrium) models, there might not be very much contaminant left in the flow by the time that equilibrium has been reached, e.g. when the loss rate λ_0 is comparable with the decay rates λ_1, λ_2 for other modes. Hence the need for two-dimensional non-equilibrium models.

4. Centroid displacement

Once $a^{(0)}$ is known, the next ingredient in the Gaussian representation (2.3*a*) is the centroid position $X(y, t; \hat{y})$. Its equation can be written

$$\partial_t(a^{(0)}X)+\alpha a^{(0)}X+\partial_y(va^{(0)}X)-\partial_y(\kappa\,\partial_y(a^{(0)}X)) = ua^{(0)}, \tag{4.1a}$$

with

$$(v-\beta_+)\,a^{(0)}X-\kappa\,\partial_y(a^{(0)}X) = 0 \quad \text{on} \quad y = y_+, \tag{4.1b}$$

$$(v+\beta_-)\,a^{(0)}X-\kappa\,\partial_y(a^{(0)}X) = 0 \quad \text{on} \quad y = y_-, \tag{4.1c}$$

and

$$a^{(0)}X = 0 \quad \text{at} \quad t = 0 \tag{4.1d}$$

(see Appendix A equation (A 1) with $m = 1$). As in the previous section we shall present solutions for small, moderate and large times after discharge.

The small-time solution for $a^{(0)}X$ is simply a multiple of the distorted Gaussian (3.2*a*). The formula for X is

$$X = tI_0/I_1+\ldots \tag{4.2a}$$

where

$$I_n = \int_{\hat{y}}^{y} \frac{u^n}{\kappa^{\frac{1}{2}}}\,\mathrm{d}y' \tag{4.2b}$$

Thus, the centroid velocity is a weighted average of the velocity profile between $\hat{y}$ and y.

To represent the right-hand side forcing term in (4.1*a*), we introduce the velocity coefficients

$$u_{mn} = \overline{u\psi_m\psi_n}, \tag{4.3a}$$

i.e.

$$ua^{(0)} = \gamma^{-\frac{1}{2}}(\hat{y})\,\gamma^{\frac{1}{2}}(y)\sum_{m=0}^{\infty}\psi_m(\hat{y})\exp(-\lambda_m t)\sum_{n=0}^{\infty}u_{mn}\psi_n(y). \tag{4.3b}$$

The composite series solution for $a^{(0)}X$ is given by

$$a^{(0)}X = \gamma^{-\frac{1}{2}}(\hat{y})\,\gamma^{\frac{1}{2}}(y)\Big\{\sum_{m=0}^{\infty}u_{mm}\,t\exp(-\lambda_m t)\,\psi_m(\hat{y})\,\psi_m(y) + \sum_{m=0}^{\infty}\sum_{n\neq m}u_{mn}J_{mn}(t)\,\psi_m(\hat{y})\,\psi_n(y)\Big\} \tag{4.4a}$$

where

$$J_{mn}(t) = \frac{\exp(-\lambda_m t)-\exp(-\lambda_n t)}{\lambda_n-\lambda_m} \tag{4.4b}$$

Barton (1984, equation following 2.13).

At large times after discharge we have the asymptote

$$a^{(0)}X = \gamma^{-\frac{1}{2}}(\hat{y})\,\gamma^{\frac{1}{2}}(y)\exp(-\lambda_0 t)\Big\{u_{00}\,t\psi_0(\hat{y})\,\psi_0(y) + \sum_{m=1}^{\infty}\frac{u_{m0}}{\lambda_m-\lambda_0}[\psi_m(\hat{y})\,\psi_0(y)+\psi_m(\hat{y})\,\psi_0(y)]\Big\}. \quad (4.5)$$

Hence, the centroid position for an elementary discharge at the level $\hat{y}$ has the limiting form

$$X \doteq u_{00}\,t+g(y)+g(\hat{y}) \quad (4.6a)$$

where

$$\psi_0(y)\,g(y) = \sum_{m=1}^{\infty}\frac{u_{m0}}{\lambda_m-\lambda_0}\psi_m(y). \quad (4.6b)$$

In Appendix B it is shown that $g(y)$ tends to be positive where $u(y)$ exceeds the asymptotic advection velocity u_{00}. As might be expected, the centroid position X tends to be displaced forwards when either the observation level y or the discharge level $\hat{y}$ is in the faster-moving part of the flow.

For later use we record the results

$$(u-u_{00})\,\psi_0(y)\,g(y) = \psi_0(y)\sum_{n=1}^{\infty}\frac{u_{n0}^2}{\lambda_n-\lambda_0} + \sum_{m=1}^{\infty}\psi_m(y)\Big[\frac{u_{m0}(u_{mn}-u_{00})}{\lambda_m-\lambda_0}+\sum_{\substack{n\neq 0\\ n\neq m}}\frac{u_{n0}\,u_{nm}}{\lambda_n-\lambda_0}\Big], \quad (4.7a)$$

$$D(\infty) = \overline{(u-u_{00})\,\psi_0^2 g} = \sum_{n=1}^{\infty}\frac{u_{n0}^2}{\lambda_n-\lambda_0}, \quad (4.7b)$$

$$\overline{\psi_0^2 g^2} = \sum_{n=1}^{\infty}\frac{u_{n0}^2}{(\lambda_n-\lambda_0)^2}. \quad (4.7c)$$

The dispersion coefficient notation $D(\infty)$ anticipates the relationship between $g(y)$ and the asymptotic growth rate of the variance σ^2 (Lungu & Moffatt 1982, equation 2.28).

The explicit solution (B 3) for $g(y)$ derived in Appendix B leads to the neat result

$$D(\infty) = \frac{1}{h}\int_{y_-}^{y_+}\frac{1}{\kappa\psi_0^2}\Big[\int_{y_-}^{y'}(u-u_{00})\,\psi_0^2\,\mathrm{d}y''\Big]^2\,\mathrm{d}y'. \quad (4.8)$$

This reveals the crucial role of the velocity shear, and the strong weighting towards parts of the flow with large ψ_0 or small κ.

5. Variance

For the variance $\sigma^2(y, t; \hat{y})$ the governing equations (A 3) can be written

$$\partial_t(a^{(0)}\sigma^2)+\alpha a^{(0)}\sigma^2+\partial_y(v a^{(0)}\sigma^2)-\partial_y(\kappa\,\partial_y(a^{(0)}\sigma^2)) = 2\kappa_L a^{(0)}+2\kappa a^{(0)}(\partial_y X)^2, \quad (5.1a)$$

with

$$(v-\beta_+)\,a^{(0)}\sigma^2-\kappa\,\partial_y(a^{(0)}\sigma^2) = 0 \quad \text{on} \quad y = y_+, \quad (5.1b)$$

$$(v+\beta_-)\,a^{(0)}\sigma^2-\kappa\,\partial_y(a^{(0)}\sigma^2) = 0 \quad \text{on} \quad y = y_-, \quad (5.1c)$$

and

$$a^{(0)}\sigma^2 = 0 \quad \text{at} \quad t = 0. \quad (5.1d)$$

Again, the small-time asymptote involves a weighted integral of the velocity profile:

$$\sigma^2 = 2t\left(\int_{\hat{y}}^{y} \frac{\kappa_L}{\kappa^{\frac{1}{2}}}\,\mathrm{d}y' \Big/ \int_{\hat{y}}^{y} \frac{\mathrm{d}y'}{\kappa^{\frac{1}{2}}}\right) + 2t^3(I_2 I_0^{-3} - I_1^2 I_0^{-4})$$

$$= 2t\kappa_L + \tfrac{1}{6}\kappa(\partial_y u)^2 t^3 \quad \text{near} \quad y = \hat{y}. \tag{5.2}$$

In practice (i.e. for high-Peclet-number flows), the timescale for transverse mixing is usually much greater than $1/\partial_y u$. Thus, the shear term rapidly overtakes the longitudinal diffusion (Townsend 1951).

To solve (5.1*a–d*) we put

$$a^{(0)}\sigma^2 = L + S - a^{(0)}(X - u_{00}t)^2, \tag{5.3}$$

where L and S respectively are associated with longitudinal diffusion and with the shear:

$$\partial_t L + \alpha L + \partial_y(vL) - \partial_y(\kappa\,\partial_y L) = 2\kappa_L a^{(0)}, \tag{5.4a}$$

$$\partial_t S + \alpha S + \partial_y(vS) - \partial_y(\kappa\,\partial_y S) = 2a^{(0)}(X - u_{00}t)(u - u_{00}). \tag{5.4b}$$

For the three-dimensional case in the absence of crossflow, there would be no counterpart of S in the expression for $a^{(0)}\sigma_3^2$.

If we introduce the notation

$$\kappa_{mn} = \overline{\kappa_L \psi_m \psi_n}, \tag{5.5}$$

then, by analogy with the solution (4.4) for $a^{(0)}X$ we have

$$L = 2\gamma^{-\frac{1}{2}}(\hat{y})\,\gamma^{\frac{1}{2}}(y)\Big\{\sum_{m=0}^{\infty} \kappa_{mm}\, t\, \exp(-\lambda_m t)\,\psi_m(\hat{y})\,\psi_m(y) + \sum_{m=0}^{\infty}\sum_{n\neq m} \kappa_{mn}\, \dot{J}_{mn}(t)\,\psi_m(\hat{y})\,\psi_n(y)\Big\}. \tag{5.6}$$

To represent the large-time asymptote we introduce the function

$$\psi_0(y)\,l(y) = \sum_{m=1}^{\infty} \frac{\kappa_{m0}}{\lambda_m - \lambda_0}\,\psi_m(y), \tag{5.7}$$

Thus, at large times

$$L \doteq 2\gamma^{-\frac{1}{2}}(\hat{y})\,\psi_0(\hat{y})\,\gamma^{\frac{1}{2}}(y)\,\psi_0(y)\,\exp(-\lambda_0 t)\,\{\kappa_{00}t + l(y) + l(\hat{y})\}. \tag{5.8}$$

The explicit formula (B 4) for $l(y)$ given in Appendix B shows that l tends to be positive where $\kappa_L(y)$ exceeds the weighted average value κ_{00}. In accord with physical intuition, this indicates that the diffusive contribution to the variance is largest when the discharge or the observations are made in that part of the flow with relatively strong longitudinal diffusivity.

To solve (5.4*b*) for $S(y, t; \hat{y})$ we pose the eigenfunction expansion

$$S = \gamma^{-\frac{1}{2}}(\hat{y})\,\gamma^{\frac{1}{2}}(y) \sum_{m=0}^{\infty} S_m(t;\hat{y})\,\psi_m(y). \tag{5.9}$$

This, together with the solutions (4.4), (3.10) for $a^{(0)}X$ and $a^{(0)}$, leads to the sequence of ordinary differential equations

$$\frac{dS_m}{dt}+\lambda_m S_m = 2(u_{mm}-u_{00})^2 t\exp(-\lambda_m t)\psi_m(\hat{y}) + 2\sum_{n\neq m}^{\infty}(u_{nn}-u_{00})u_{mn}t\exp(-\lambda_n t)\psi_n(\hat{y}) + 2\sum_{\substack{n=0\\ n\neq m}}^{\infty}(u_{mm}-u_{00})u_{mn}J_{mn}(t)\psi_n(\hat{y}) + 2\sum_{\substack{l=0\\ l\neq m}}^{\infty}\sum_{n\neq l}u_{nl}u_{ml}\left[\frac{\exp(-\lambda_l t)-\exp(-\lambda_n t)}{\lambda_n-\lambda_l}\right]\psi_n(\hat{y}). \quad (5.10)$$

The solutions for the eigen-coefficients $S_m(t;\hat{y})$ are

$$S_m = (u_{mm}-u_{00})^2 t^2\exp(-\lambda_m t)\psi_m(\hat{y}) - 2\sum_{n\neq m}^{\infty}\frac{(u_{nn}-u_{00})u_{mn}}{\lambda_n-\lambda_m}[t\exp(-\lambda_n t)-J_{mn}(t)]\psi_n(\hat{y}) + 2\sum_{\substack{n=0\\ n\neq m}}^{\infty}\frac{(u_{mm}-u_{00})u_{mn}}{\lambda_n-\lambda_m}[t\exp(-\lambda_m t)-J_{mn}(t)]\psi_n(\hat{y}) + 2\sum_{\substack{l=0\\ l\neq m}}^{\infty}\sum_{n\neq m}\frac{u_{nl}u_{ml}}{\lambda_n-\lambda_l}\{J_{ml}(t)-J_{mn}(t)\}\psi_n(\hat{y}) + 2\sum_{\substack{l=0\\ l\neq m}}\frac{u_{ml}^2}{\lambda_l-\lambda_m}[t\exp(-\lambda_m t)-J_{ml}(t)]\psi_m(\hat{y}). \quad (5.11)$$

At large times after discharge we have the asymptotes

$$S_0 \doteq 2\exp(-\lambda_0 t)\left\{t\sum_{l=1}^{\infty}\frac{u_{0l}^2}{\lambda_l-\lambda_0}-\sum_{l=1}^{\infty}\frac{u_{0l}^2}{(\lambda_l-\lambda_0)^2}\right\}\psi_0(\hat{y}) + 2\exp(-\lambda_0 t)\left\{\sum_{n=1}^{\infty}\psi_n(\hat{y})\left[\frac{(u_{nn}-u_{00})u_{0n}}{(\lambda_n-\lambda_0)^2}+\sum_{\substack{l=1\\ l\neq n}}\frac{u_{nl}u_{0l}}{(\lambda_n-\lambda_0)(\lambda_l-\lambda_0)}\right]\right\} \quad (5.12a)$$

$$S_m \doteq 2\exp(-\lambda_0 t)\psi_0(\hat{y})\left[\frac{(u_{mm}-u_{00})u_{0m}}{(\lambda_m-\lambda_0)^2}+\sum_{\substack{l\neq 0\\ l\neq m}}^{\infty}\frac{u_{ml}u_{0l}}{(\lambda_l-\lambda_0)(\lambda_m-\lambda_0)}\right] + 2\exp(-\lambda_0 t)\sum_{\substack{n\neq 0\\ n\neq m}}\frac{u_{n0}u_{m0}}{(\lambda_n-\lambda_0)(\lambda_m-\lambda_0)}\psi_n(\hat{y}) \quad (m>0). \quad (5.12b)$$

By analogy with the definition (4.6b) of $g(y)$, we define

$$\psi_0(y)g^{(2)}(y) = \sum_{m=1}^{\infty}\psi_m(y)\left[\frac{(u_{mm}-u_{00})u_{0m}}{(\lambda_m-\lambda_0)^2}+\sum_{\substack{l=1\\ l\neq m}}\frac{u_{ml}u_{0l}}{(\lambda_l-\lambda_0)(\lambda_m-\lambda_0)}\right]. \quad (5.13)$$

Also, for later use we define

$$R(y) = g^{(2)}(y)-\tfrac{1}{2}[g(y)^2-\overline{\psi_0^2 g^2}], \quad (5.14a)$$

where
$$\overline{\psi_0^2 R} = 0. \tag{5.14b}$$

An integral expression for $R(y)$ is given in Appendix B.

In terms of g and $g^{(2)}$, the second moment, $S(y, t; \hat{y})$ has the asymptote

$$S \doteq 2\gamma^{-\frac{1}{2}}(\hat{y})\,\psi_0(\hat{y})\,\gamma^{\frac{1}{2}}(y)\,\psi_0(y)\exp(-\lambda_0 t)$$
$$\{tD(\infty) - \overline{\psi_0^2 g^2} + g^{(2)}(\hat{y}) + g^{(2)}(y) + g(y)\,g(\hat{y})\}. \tag{5.15}$$

Combining together the asymptotic results (3.11, 4.6*a*, 5.8, 5.15) we can infer that the variance $\sigma^2(y, t; \hat{y})$ has the asymptote

$$\sigma^2 \doteq 2t[D(\infty) + \kappa_{00}] - 3\overline{\psi_0^2 g^2} + 2R(y) + 2l(y) + 2R(\hat{y}) + 2l(\hat{y}). \tag{5.16}$$

For high-Peclet-number flows the diffusive contributions to the variance are dominated by the shear terms. Thus, to compare the amount of spreading for different discharge heights $\hat{y}$ it suffices to calculate just the single function $R(\hat{y})$. The symmetry between y and $\hat{y}$ is absent in the results of Smith (1982, equation 4.16) and of Barton (1984, equation 2.22) due to their having focused attention upon cross-sectionally averaged discharges and concentrations respectively. It deserves emphasis that in Appendix B all the quantities in (5.16) are given explicitly in terms of integrals involving the lowest mode $\psi_0(y)$, the diffusivities $\kappa(y)$, $\kappa_L(y)$, and the velocity profile $u(y)$.

6. Open-channel flow with retention at the bed

For turbulent open-channel flow the velocity and diffusivity profiles can be modelled as

$$u = \bar{u} + \frac{u_*}{k}[1 + \ln\eta] = \frac{u_*}{k}\ln\left[\frac{\eta}{\eta_*}\right], \tag{6.1a}$$

$$\kappa = khu_*\,\eta(1-\eta), \tag{6.1b}$$

with

$$\eta = \eta_* + \left(1 + \frac{y}{h}\right)(1-\eta_*), \tag{6.1c}$$

$$u_* = \frac{k\bar{u}}{\left[\ln\left(\frac{1}{\eta_*}\right) - 1\right]}. \tag{6.1d}$$

Here $\bar{u}$ is the bulk velocity, u_* the friction velocity, k von Kármán's constant (about 0.4), h the water depth, and η_* a dimensionless roughness height. Typically u_* is about $\frac{1}{15}\bar{u}$, which implies that η_* is about 0.001. Motivated by the application to accidental discharges of long-lived radioactive isotopes from storage tanks, we take the settling velocity $-v$, the decay rate α, and the free-surface absorption coefficient β_+ all to be negligibly small. Hence, we focus our attention upon the effects of retention at the bed.

If we ignore terms of order η_*, then the field equation (3.8*a*) for the eigenmodes transforms to

$$\eta(1-\eta)\frac{\mathrm{d}^2\psi_m}{\mathrm{d}\eta^2} + (1-2\eta)\frac{\mathrm{d}\psi_m}{\mathrm{d}\eta} + \mu_m\psi_m = 0, \tag{6.2a}$$

with

$$\lambda_m = \mu_m\frac{ku_*}{h}. \tag{6.2b}$$

In the limit of zero roughness, we can ignore the boundary conditions (3.8*b*, *c*) and the solutions are Legendre polynomials:

$$\psi_m^{(0)} = (2m+1)^{\frac{1}{2}} P_m(2\eta-1), \quad \mu_m^{(0)} = m(m+1), \tag{6.3a, b}$$

$$u_{00}^{(0)} = \bar{u}, \quad u_{m0}^{(0)} = (-1)^{m+1} \frac{u_*}{k} \frac{(2m+1)^{\frac{1}{2}}}{m(m+1)}, \tag{6.3c, d}$$

$$u_{mm}^{(0)} - u_{00}^{(0)} = -\frac{u_*}{k}\left[-\frac{2m}{2m+1} + \frac{1}{2}\sum_{j=1}^{m} \frac{1}{(j-\frac{1}{2})j}\right], \tag{6.3e}$$

$$u_{mn}^{(0)} = \frac{u_*}{k}(-1)^{n+m+1} \frac{(2n+1)^{\frac{1}{2}}(2m+1)^{\frac{1}{2}}}{|n-m|(n+m+1)} \tag{6.3f}$$

(Smith 1981*a*, §9).

To leading order the boundary condition at the bed is

$$ku_* \eta_* \frac{\mathrm{d}\psi_m}{\mathrm{d}\eta} = \beta\psi_m \quad \text{at} \quad \eta = \eta_*. \tag{6.4}$$

This can be accommodated if we add the correction terms

$$\psi_m^{(1)} = \frac{u_*}{k\bar{u}} \frac{B}{1+B}\left\{[1+\ln\eta]\psi_m^{(0)} - k\frac{(u_{mm}^{(0)} - \bar{u})}{u_*}\psi_m^{(0)} - 2\sum_{n=0}^{m-1} \frac{ku_{mn}^{(0)}}{u_*}\psi_n^{(0)}\right\}, \tag{6.5a}$$

$$\mu_m^{(1)} = \frac{u_*}{k\bar{u}} \frac{B}{1+B}(2m+1), \tag{6.5b}$$

with

$$B = \frac{\beta\bar{u}}{u_*^2}. \tag{6.5c}$$

As is indicated by the logarithmic term in (6.5*a*), the effects of boundary absorption are predominantly local to the bed. Thus, there are only small changes to such global parameters as u_{00}, u_{m0}, u_{mm}, u_{mn}. For example,

$$u_{00}^{(1)} = \bar{u}\left[\frac{u_*}{k\bar{u}}\right]^2 \frac{B}{1+B}. \tag{6.6}$$

which shows that the removal of contaminant near the bed has the consequence of very slightly increasing the asymptotic centroid velocity (at most by less than 3%).

An important exception is the asymptotic loss rate:

$$\lambda_0 = \frac{u_*^2}{h\bar{u}} \frac{B}{1+B} \tag{6.7}$$

(see figure 1). No matter how small the value of λ_0, at sufficiently large times after discharge it is this loss rate that determines the amount of contaminant remaining in the flow. In the limit of total retention ($B \to \infty$) the *e*-folding time corresponds to a distance $(\bar{u}/u_*)^2 h$ downstream i.e. about 225 times the water depth. This is about 12 times further than the *e*-folding distance for the decay of the higher modes, and for the vertical concentration to have become uniform. At such large distances, the present two-dimensional description of the concentration field is unnecessarily complicated, and a one-dimensional model would suffice.

Figure 2 shows the composite lowest mode $\psi_0^{(0)} + \psi_0^{(1)}$ for $u_*/\bar{u} = \frac{1}{15}$. The similarity between ψ_0 and the logarithmic velocity profile (6.1*a*) is by no means accidental. The model (6.1*b*) for κ is based upon Reynolds' hypothesis that the eddy diffusivities for mass and for momentum are equal. In view of the results (3.11) and (3.12) we infer

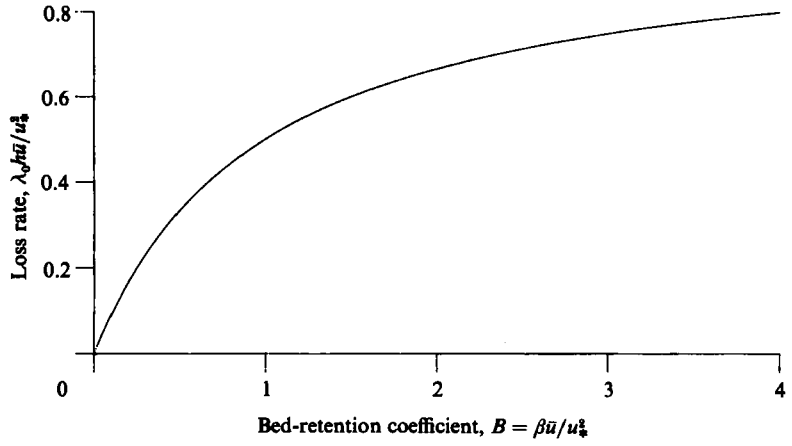

FIGURE 1. The dependence of the asymptotic depletion rate λ_0 upon the retention of the bed β in turbulent open-channel flow.

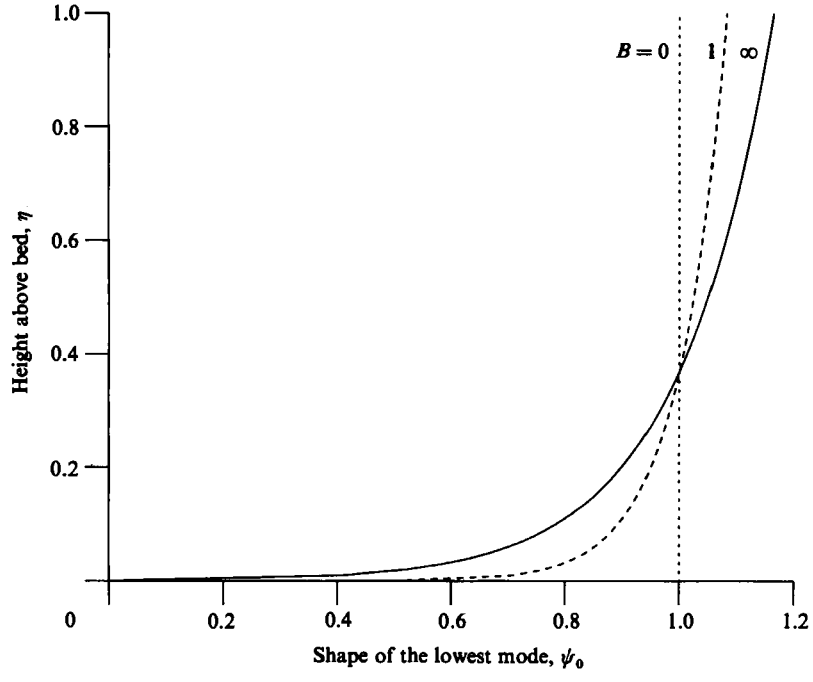

FIGURE 2. The lowest mode ψ_0 when the non-dimensional bed-retention coefficient $B = \beta\bar{u}/u_*^2$ has the values $B = 0$ (.....); 1 (----); ∞ (——); with $u_*/\bar{u} = \frac{1}{15}$. This can be interpreted as showing the shape of the asymptotic concentration profile, or as the dependence of the total amount of contaminant remaining in the flow upon the discharge height.

that at large times the total amount of contaminant remaining in the fluid is not sensitive to the precise discharge height unless the discharge is extremely close to the bed. At the bed itself we have the neat result

$$\psi_0^{(0)} + \psi_0^{(1)} = \frac{1}{(1+B)} \quad \text{on} \quad \eta = \eta_*. \tag{6.8}$$

To a first approximation this same reduction factor applies to the higher modes, and hence to the entire concentration field.

7. Open-channel flow with gravitational settling

A simple model for the mixing of fine-grained sediments is to consider dispersion in open-channel flow when there is a constant vertical drift velocity v. This class of problem is also of interest in the context of waste disposal, and again comes under the general framework established in the first half of the present paper. Absorption at the bed or through the free surface will be ignored, and the reaction rate α taken to be constant or zero.

The reference profile $\gamma(y)$ is given by

$$\gamma = \frac{1}{\Gamma(1+V)\,\Gamma(1-V)}\left[\frac{\eta}{1-\eta}\right]^V = \frac{\sin\pi V}{\pi V}\left[\frac{\eta}{1-\eta}\right]^V \tag{7.1a}$$

with

$$V = \frac{v}{ku_*} \tag{7.1b}$$

The normalization for γ involves a beta-function, which can be expressed in terms of gamma functions, and finally written as above with the sine function (Abramowitz & Stegun 1965, §6.2). Near the boundaries the balance between vertical diffusion and drift is possible only for the non-dimensional velocity V in the range $(-1, 1)$. Figure 3 illustrates how the contaminant accumulates towards the upper or lower boundary accordingly as the vertical drift velocity is upwards or downwards.

If we remove an additional factor of $\gamma^{\frac{1}{2}}$, then the field equation (3.8a) for the eigenmodes takes the form

$$\eta(1-\eta)\frac{\mathrm{d}^2\phi_m}{\mathrm{d}\eta^2} + (1+V-2\eta)\frac{\mathrm{d}\phi_m}{\mathrm{d}\eta} + \mu_m\phi_m = 0 \tag{7.2a}$$

where

$$\psi_m(\eta) = \gamma^{\frac{1}{2}}(\eta)\,\phi_m(\eta), \quad \lambda_m = \alpha + \mu_m\frac{ku_*}{h} \tag{7.2b, c}$$

In the limit of zero roughness the solutions for ϕ_m are Jacobi polynomials (Abramowitz & Stegun 1965, chapter 22)

$$\phi_m = \frac{P_m^{(-V,\,V)}(2\eta-1)\,(2m+1)^{\frac{1}{2}}}{\prod_{j=1}^{m}\left[1-\frac{V^2}{j^2}\right]^{\frac{1}{2}}}, \tag{7.3a}$$

$$\mu_m = m(m+1). \tag{7.3b}$$

For zero drift velocity this is identical to the leading-order solution given in (6.3a, b) above.

If the appropriate beta-function integral is differentiated with respect to one of its arguments, we can then obtain the logarithmic integral $\overline{u\gamma}$ for the asymptotic centroid velocity u_{00}. The derivative of a beta function can be expressed in terms of digamma functions (Abramowitz & Stegun 1965, §6.3). A numerically useful form of the final expression for u_{00} is

$$u_{00} - \bar{u} = \frac{u_*}{k}\left\{\frac{1}{2V} - \frac{\pi}{2}\cot\pi V - \frac{V^2}{1-V^2} - \sum_{n=1}^{\infty}\left[\zeta(2n+1)-1\right]V^2\right\}, \tag{7.4a}$$

with

$$\left.\begin{aligned}\zeta(3) &= 1.20205, \quad \zeta(5) = 1.03692, \quad \zeta(7) = 1.00834,\\ \zeta(9) &= 1.00200, \quad \zeta(11) = 1.00049, \quad \zeta(13) = 1.00012,\end{aligned}\right\} \tag{7.4b}$$

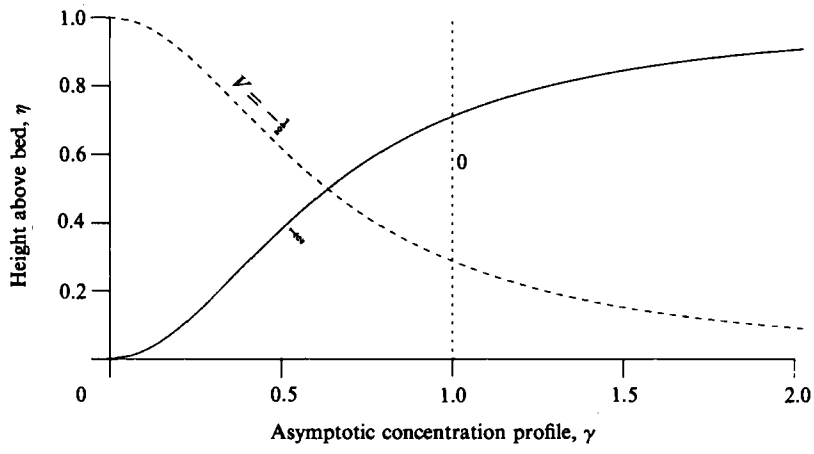

FIGURE 3. The equilibrium concentration profile across the flow for upwards (——), zero (.....), and downwards (– – –) drift velocities.

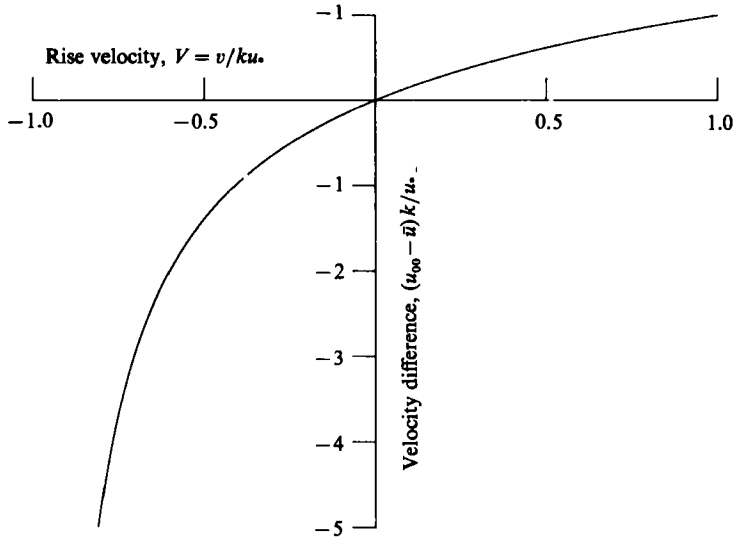

FIGURE 4. The dependence of the asymptotic advection velocity u_{00} upon the vertical drift velocity.

where $\zeta(n)$ denotes the Riemann zeta function (Abramowitz & Stegun 1965, table 23.3). Figure 4 shows the departure of u_{00} from the bulk velocity $\bar{u}$ as a function of V. For $V > 0$ the contaminant has a tendency to rise and to occupy the faster-moving part of the flow, with the consequence that the weighted average advection velocity $u_{00} = \overline{u\gamma}$ exceeds $\bar{u}$. Conversely, when $V < 0$ the advection velocity is less than $\bar{u}$, with a marked decrease as the contaminant becomes more closely confined to the bed.

To evaluate the coefficients u_{m0} in the series (4.6*b*, 4.7*b*) for $g(y)$ and $D(\infty)$, we employ the Rodrigues' formula for Jacobi polynomials (Abramowitz & Stegun 1965, 22.11.1). Integration by parts m times then yields

$$u_{m0} = (-1)^{m+1} \frac{u_*}{k} \frac{(2m+1)^{\frac{1}{2}}}{m(m+1)} \prod_{j=1}^{m} \left[\frac{j-V}{j+V}\right]^{\frac{1}{2}}. \tag{7.5}$$

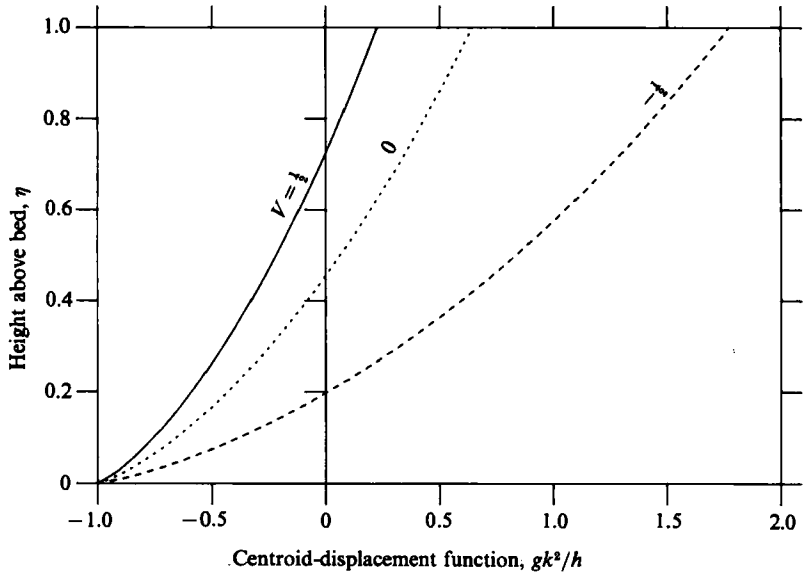

FIGURE 5. The dependence $g(\eta)$ of the centroid displacement upon the discharge height when there is upwards (——), zero (.....), and downwards (– – – –) drift velocities.

At the bed, the V-dependence of the modes $\phi_m^{(0)}$ exactly counterbalances that of the u_{m0} weights, leaving the centroid displacement function $g(0)$ independent of the vertical drift. However, away from the bed the role of the u_{m0} coefficients predominates. Thus the centroid displacement is more sensitive to the discharge height (or observation level) when the contaminant tends to sink (see figure 5). Likewise, the asymptotic shear-dispersion coefficient $D(\infty)$ is larger when the contaminant profile across the flow is weighted towards the bed, where the shear is greatest (see figure 6).

The algebraic integrals (16.4.5, 16.4.10) stated by Erdelyi *et al.* (1954) are a convenient starting point for the derivation of the higher-order diagonal velocity coefficients u_{mm}. The required logarithmic factor can be introduced by differentiation with respect to the superscripts of the Jacobi Polynomials. The differentiation of gamma functions leads to the occurrence of digamma functions. However, these conveniently cancel when we subtract u_{00}:

$$u_{mm}-u_{00} = -\frac{u_*}{k}\left[\frac{-2m}{2m+1}+(\tfrac{1}{2}+V)\sum_{j=1}^{m}\frac{1}{(j-\tfrac{1}{2})(j+V)}\right]. \tag{7.6}$$

For the off-diagonal velocity coefficients the starting point is the corrected version of equation (16.4.12) of Erdelyi *et al.* (1954). This time digamma functions do not arise, and the final expression is

$$u_{mn} = \frac{u_*}{k}(-1)^{n+m+1}\frac{(2n+1)^{\frac{1}{2}}(2m+1)^{\frac{1}{2}}}{|n-m|(n+m+1)}\prod_{\min(n,\,m)+1}^{\max(m,\,n)}\left[\frac{j-V}{j+V}\right]^{\frac{1}{2}}. \tag{7.7}$$

A guiding principle throughout the evaluation of the formidable integrals was that the form of the result was known in the case $V = 0$ (see 6.3c–f).

Armed with the values of these coefficients u_{00}, u_{m0}, $u_{mm}-u_{00}$, u_{mn} and secure in the knowledge that shear dispersion does indeed dominate longitudinal dispersion κ_L for open-channel flow (Elder 1959), we can make full use of the results derived in the first half of this paper. For example, figure 7 gives the variance function $R(\eta)$. As

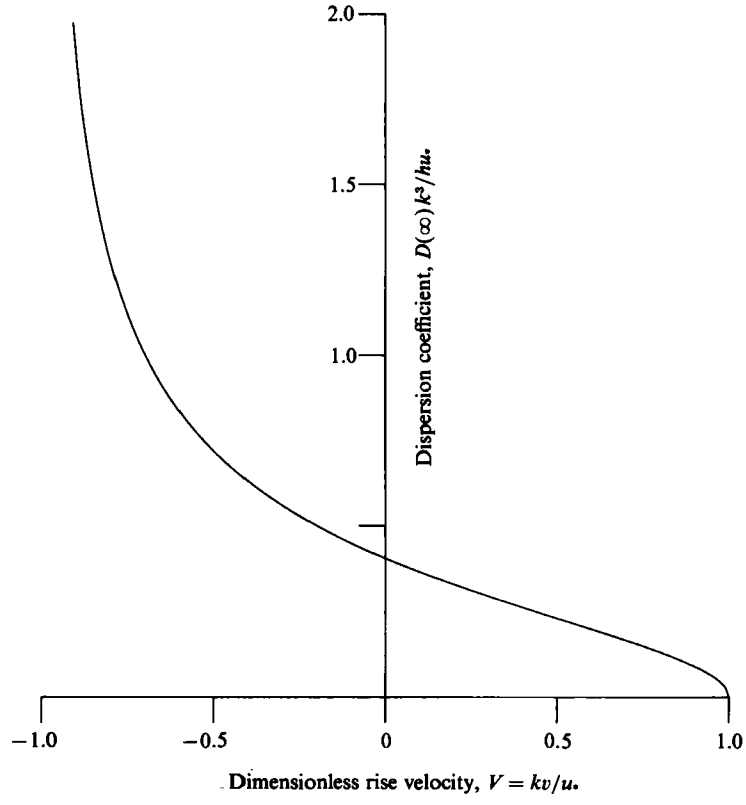

FIGURE 6. The dependence of the shear-dispersion coefficient $D(\infty)$ upon the vertical drift velocity.

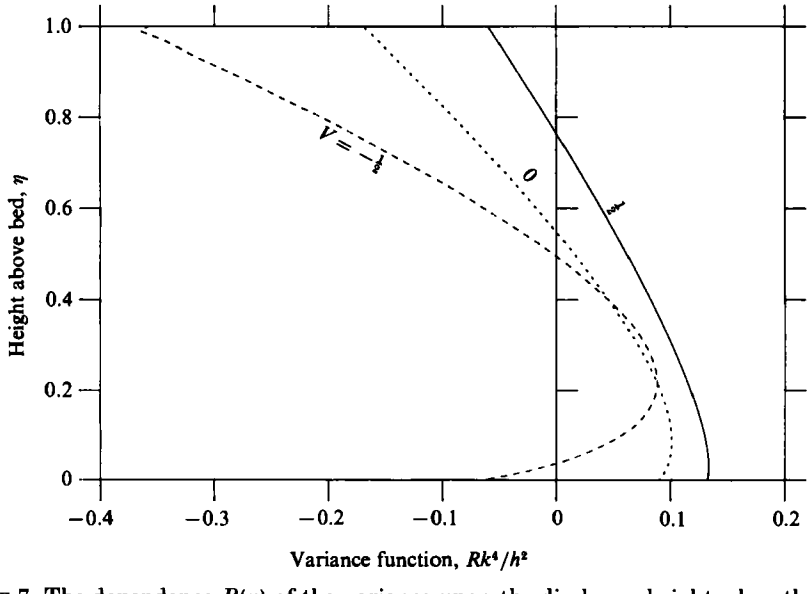

FIGURE 7. The dependence $R(\eta)$ of the variance upon the discharge height when there is upwards (——), zero (.....) and downwards (– – –) drift velocities.

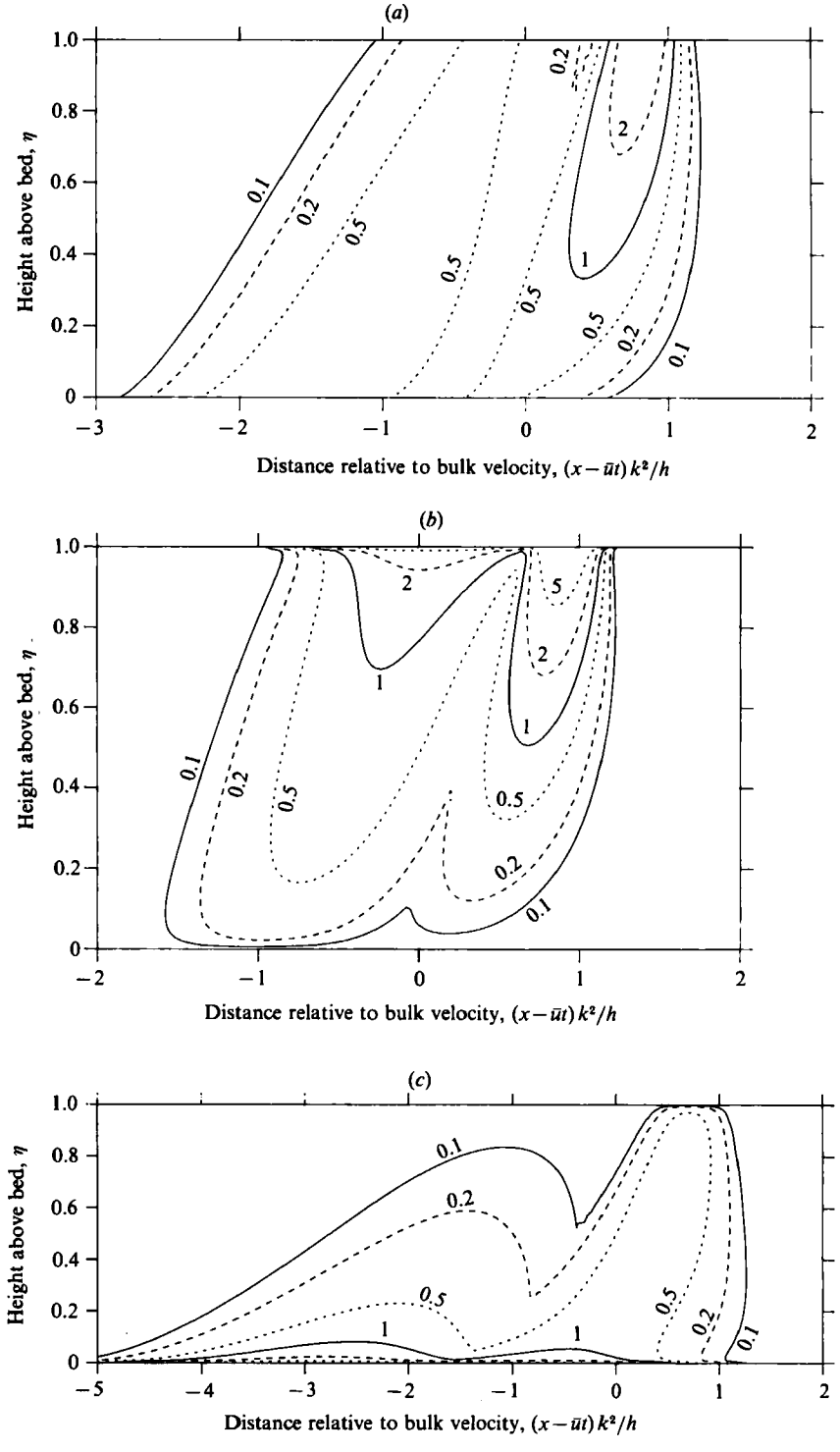

FIGURE 8. Concentration contours for surface and for bed discharges (*a*) with zero vertical drift $V = 0$, (*b*) with upwards drift $V = \frac{1}{2}$, and (*c*) with downwards drift $V = -\frac{1}{2}$.

was the case for the centroid displacement $g(\eta)$, the value of $R(\eta)$ tends to be larger and the sensitivity to the discharge height most marked when there is downwards drift. We note that, unlike the results at a fixed distance downstream (Smith 1981*b*), at a fixed time after discharge the variance is maximized for a discharge just above the bed.

To illustrate the importance of source position, figure 8(*a*) shows the Gaussian approximation to the concentration for surface and for bed discharges in the case

$$V = 0, \quad \alpha = 0, \quad t = \frac{h}{ku_*}. \tag{7.8}$$

The lateral separation of the two contaminant clouds is sufficient to permit their inclusion on the same figure without significant overlap, though the time is too short for the large-time asymptotes to be utilised. (The contours show the larger of the two concentrations.) The additional effect of vertical drift is included in figures 8(*b*, *c*) where the non-dimensional rise velocity V has the respective values $\frac{1}{2}$, $-\frac{1}{2}$. In all cases the concentrations are significantly smaller when the discharge is made at the bed.

The author is grateful to the Royal Society for financial support.

Appendix A. Hermite series

An appropriate choice for the centroid and variance functions X and σ^2 ensures that the Gaussian approximation (2.2*a*) exactly reproduces the zero, first and second moments of c with respect to x. However, the third and higher moments are not exact (skewness, kurtosis, ...). This can be remedied by the inclusion of additional terms:

$$c = \int_{y_-}^{y_+} \mathrm{d}\hat{y}\, \frac{q(\hat{y})}{(2\pi)^{\frac{1}{2}}\sigma} \exp(-\tfrac{1}{2}\xi^2)\left\{a^{(0)} + \sum_{m=3}^{\infty} \frac{a^{(m)}}{\sigma^m} \mathrm{He}_m(\xi)\right\} \tag{A 1a}$$

with

$$\xi = \frac{x - X}{\sigma}. \tag{A 1b}$$

The Hermite functions $\mathrm{He}_m(\xi)$ can be defined inductively

$$\mathrm{He}_0 = 1, \quad \mathrm{He}_1 = \xi, \quad \mathrm{He}_{m+2} = \xi\, \mathrm{He}_{m+1} - (m+1)\, \mathrm{He}_m. \tag{A 2}$$

The equations satisfied by the coefficients $a^{(0)}$, X, σ^2, $a^{(3)}$, ..., can be obtained by substituting the representation (A 1*a*) into the field equation (2.1*a*) and extracting the coefficients of He_m:

$$\begin{aligned}
&\partial_t a^{(m)} + \alpha a^{(m)} + \partial_y(v a^{(m)}) - \partial_y(\kappa\, \partial_y a^{(m)}) \\
&\quad = (u - \partial_t X - v\, \partial_y X)\, a^{(m-1)} + \kappa\, \partial_y X\, \partial_y a^{(m-1)} + \partial_y(\kappa a^{(m-1)}\, \partial_y X) \\
&\quad + \tfrac{1}{2}\{(2\kappa_L - \partial_t \sigma^2 - v\, \partial_y \sigma^2)\, a^{(m-2)} + \kappa\, \partial_y \sigma^2\, \partial_y a^{(m-2)} \\
&\quad + \partial_y(\kappa a^{(m-2)}\, \partial_y \sigma^2) + 2\kappa(\partial_y X)^2 a^{(m-2)}\} + \kappa\, \partial_y X \partial_y \sigma^2 a^{(m-3)} + \tfrac{1}{4}\kappa(\partial_y \sigma^2)^2 a^{(m-4)},
\end{aligned} \tag{A 3a}$$

with

$$(v - \beta_+)\, a^{(m)} - \kappa\, \partial_y a^{(m)} = a^{(m-1)} \kappa\, \partial_y X + \tfrac{1}{2} a^{(m-2)} \kappa\, \partial_y \sigma^2 \quad \text{on} \quad y = y_+ \tag{A 3b}$$

$$(v + \beta_-)\, a^{(m)} - \kappa\, \partial_y a^{(m)} = a^{(m-1)} \kappa\, \partial_y X + \tfrac{1}{2} a^{(m-2)} \kappa\, \partial_y \sigma^2 \quad \text{on} \quad y = y_-, \tag{A 3c}$$

and

$$a^{(0)} = \delta(y - \hat{y}), \quad X = 0, \quad \sigma^2 = 0, \quad a^{(m)} = 0 \quad \text{at} \quad t = 0. \tag{A 3d}$$

The feature of the representation (A 1a, b) which distinguishes it from the author's earlier work (Smith 1982) is the inclusion of the $\hat{y}$-dependence. The way that this has been done, with X, σ^2 and $a^{(m)}$ all functions of $\hat{y}$, ensures that the solution preserves the linear superposition property for varied discharge distributions $q(\hat{y})$. Unfortunately, this makes the solution cumbersome for uniform discharges, but economical for point discharges. Thus, the numerical examples given at the end of the above paper all concern point discharges.

Barton (1984) follows upon the passive contaminant work of Chatwin (1970), and uses a Hermite-series representation with σ^2 independent of y. This is appropriate for large times after discharge, which is indeed the aspect of particular concern to Barton (1984). However, at moderate times the marked dependence of the variance upon y (Smith 1982, figures 2a, 5a) makes this approach inefficient, with additional and large $a^{(1)}$, $a^{(2)}$ coefficients in the series (A 1a).

Appendix B. Formulae for the centroid and variance functions

The eigenfunction expansion (4.6b) makes it difficult to see the relationship between the centroid displacement function $g(y)$ and the velocity profile $u(y)$. However, making use of the (3.8a–e) satisfied by the eigenfunctions $\psi_m(y)$ we can deduce that $g(y)$ is solution of the vertical diffusion equation

$$\frac{\mathrm{d}}{\mathrm{d}y}\left[\kappa\psi_0^2\frac{\mathrm{d}g}{\mathrm{d}y}\right] = (u_{00}-u(y))\,\psi_0(y)^2, \tag{B 1a}$$

with

$$\kappa\psi_0^2\,\partial_y g = 0 \quad \text{on} \quad y = y_+, y_-, \tag{B 1b}$$

and

$$\overline{g\psi_0^2} = 0. \tag{B 1c}$$

In the notation of Lungu & Moffatt (1982) $F_{01} = \psi_0 g$, and the above equations for $g(y)$ are equivalent to their equations (2.22, 2.24).

The boundary conditions (B 1b) make it possible to integrate (B 1a) once to get a formula for $\partial_y g$. A second integration compatible with the constraint (B 1c) requires more subtlety. If we introduce the functions (Smith 1981b, §5)

$$p_+(y) = \frac{1}{h}\int_y^{y_+}\psi_0^2\,\mathrm{d}y, \quad p_- = \frac{1}{h}\int_{y_-}^{y}\psi_0^2\,\mathrm{d}y, \quad p_+ + p_- = 1, \tag{B 2}$$

then the solution for $g(y)$ can be shown to be

$$g = \int_y^{y_+}\frac{p_+(y')}{\kappa\psi_0^2}\left[\int_{y_-}^{y'}(u-u_{00})\,\psi_0^2\,\mathrm{d}y''\right]\mathrm{d}y' + \int_{y_-}^{y}\frac{p_-(y)}{\kappa\psi_0^2}\left[\int_{y'}^{y_+}(u-u_{00})\,\psi_0^2\,\mathrm{d}y'\right]\mathrm{d}y'. \tag{B 3}$$

It follows that $g(y)$ tends to be positive where $u(y)$ exceeds the asymptotic advection velocity u_{00}.

For the function $l(y)$ defined by the eigenfunction expansion (5.7), the role of the velocity coefficients u_{m0} is taken over by the longitudinal diffusivity coefficients κ_{m0}. By direct analogy with the above solution for $g(y)$ we conclude that

$$l = \int_y^{y_+}\frac{p_+(y')}{\kappa\psi_0^2}\left[\int_{y_-}^{y'}(\kappa-\kappa_{00})\,\psi_0^2\,\mathrm{d}y''\right]\mathrm{d}y' + \int_{y_-}^{y}\frac{p_-(y')}{\kappa\psi_0^2}\left[\int_{y'}^{y_+}(\kappa-\kappa_{00})\,\psi_0^2\,\mathrm{d}y''\right]\mathrm{d}y'. \tag{B 4}$$

Making use of the results (4.7*a*, *b*), we can verify that $g^{(2)}(y)$, as defined by the eigenfunction expansion (5.13), satisfies the vertical diffusion equation

$$\frac{\mathrm{d}}{\mathrm{d}y}\left[\kappa\psi_0^2\frac{\mathrm{d}}{\mathrm{d}y}g^{(2)}\right] = \psi_0^2\overline{[(u-u_{00})\psi_0^2 g-(u-u_{00})g]}, \tag{B 5a}$$

with

$$\kappa\psi_0^2\partial_y g^{(2)} = 0 \quad \text{on} \quad y = y_+, y_- \tag{B 5b}$$

and

$$\overline{g^{(2)}\psi_0^2} = 0. \tag{B 5c}$$

Instead of solving for $g^{(2)}(y)$, we shall go on to consider the closely related, but physically more important, function $R(y)$ defined by (5.14*a*). From the diffusion equations (B 1*a*, B 5*a*) and the solution (B 3) for $g(y)$, we infer that

$$\frac{\mathrm{d}}{\mathrm{d}y}\left[\kappa\psi_0^2\frac{\mathrm{d}R}{\mathrm{d}y}\right] = D(\infty)\psi_0^2-\frac{1}{\kappa\psi_0^2}\left[\int_{y_-}^{y}(u-u_{00})\,\mathrm{d}y'\right]^2, \tag{B 6a}$$

with

$$\kappa\psi_0^2\partial_y R = 0 \quad \text{on} \quad y = y_+, y_-, \tag{B 6b}$$

and

$$\overline{R\psi_0^2} = 0. \tag{B 6c}$$

If we define (cf. Smith 1981*b*, equation 5.10)

$$D_+(y) = \frac{1}{h}\int_y^{y_+}\frac{1}{\kappa\psi_0^2}\left[\int_{y'}^{y_+}(u-u_{00})\,\psi_0^2\,\mathrm{d}y''\right]^2\mathrm{d}y' \tag{B 7a}$$

$$D_-(y) = \frac{1}{h}\int_{y_-}^{y}\frac{1}{\kappa\psi_0^2}\left[\int_{y_-}^{y'}(u-u_{00})\,\psi_0^2\,\mathrm{d}y''\right]^2\mathrm{d}y' \tag{B 7b}$$

(i.e. y-dependent counterparts to the formula (4.8) for $D(\infty)$), then a first integral for equations (B 6*a*, *b*) is

$$\frac{\kappa\psi_0^2}{h}\frac{\mathrm{d}R}{\mathrm{d}y} = D(\infty)\,p_-(y)-D_-(y) = D_+(y)-D(\infty)\,p_+(y). \tag{B 8}$$

In general, we can expect the single integral $p_-(y)$ to grow more rapidly away from the boundary $y = y_-$ than does the repeated integral $D_-(y)/D(\infty)$. Thus, $R(y)$ would be increasing and the variance σ^2 will be larger for discharges away from the boundary. The second integral for equations (B 6*a*, *b*), compatible with the constraint (B 6*c*) can be written

$$R(y) = h\int_{y_-}^{y}\frac{D_+p_-}{\kappa\psi_0^2}\,\mathrm{d}y'+h\int_y^{y_+}\frac{D_-p_+}{\kappa\psi_0^2}\,\mathrm{d}y'-D(\infty)\,h\int_{y_-}^{y_+}\frac{p_+p_-}{\kappa\psi_0^2}\,\mathrm{d}y'. \tag{B 9}$$

REFERENCES

Abramowitz, M. & Stegun, I. A. 1965 *Handbook of Mathematical Functions*. Dover.

Barton, N. G. 1984 An asymptotic theory for dispersion of reactive contaminants in parallel flow. *J. Austral. Math. Soc.* B **25**, 287–310.

Chatwin, P. C. 1970 The approach to normality of the concentration distribution of a solute in a solvent flowing along a straight pipe. *J. Fluid Mech.* **43**, 321–352.

Doshi, M. R., Gill, W. N. & Subramanian, R. S. 1975 Unsteady reverse osmosis or ultrafiltration in a tube. *Chem. Engng Sci.* **30**, 1467–1476.

Elder, J. S. 1959 The dispersion of marked fluid in turbulent shear flow. *J. Fluid Mech.* **5**, 544–560.

ERDELYI, A., MAGNUS, W., OBERHETTINGER, F. & TRICOMI, F. G. 1954 *Tables of Integral Transforms*, vol. 2. McGraw Hill.

FISCHER, H. B., LIST, E. J., KOH, R. C. Y., IMBERGER, J. & BROOKS, N. H. 1979 *Mixing in Inland and Coastal Waters*. Academic.

HSIEH, H. P., LEE, G. Y. & GILL, W. N. 1979 Interfacial transport of energy in laminar open-channel and film flows. *Chem. Engng Commun.* **3**, 105–124.

JAYARAJ, K. & SUBRAMANIAN, R. S. 1978 On relaxation phenomena in field-flow separation. *Sep. Sci. Tech.* **130**, 791–817.

KRISHNAMURTHY, S. & SUBRAMANIAN, R. S. 1977 Exact analysis of field-flow fractionation. *Sep. Sci. Tech.* **12**, 347–379.

LUNGU, E. M. & MOFFATT, H. K. 1982 The effect of wall conductance on heat diffusion in duct flow. *J. Engng Maths* **16**, 121–136.

SANKARASUBRAMANIAN, R. & GILL, W. N. 1973 Unsteady convective diffusion with interface mass transfer. *Proc. R. Soc. Lond.* A **333**, 115–132.

SANKARASUBRAMANIAN, R. & GILL, W. N. 1975 Correction to 'Unsteady convective diffusion with interface mass transfer'. *Proc. R. Soc. Lond.* A **341**, 407–408.

SMITH, R. 1981*a* A delay-diffusion description for contaminant dispersion. *J. Fluid Mech.* **105**, 469–486.

SMITH, R. 1981*b* The importance of discharge siting upon contaminant dispersion in narrow rivers and estuaries. *J. Fluid Mech.* **108**, 43–53.

SMITH, R. 1982 Gaussian approximation for contaminant dispersion. *Q. J. Mech. Appl. Maths* **35**, 345–366.

SMITH, R. 1983*a* Field-flow fractionation. *J. Fluid Mech.* **129**, 347–364.

SMITH, R. 1983*b* Effect of boundary absorption upon longitudinal dispersion in shear flows. *J. Fluid Mech.* **134**, 161–177.

SULLIVAN, P. J. 1971 Longitudinal dispersion within a two-dimensional turbulent shear flow. *J. Fluid Mech.* **49**, 551–576.

TOWNSEND, A. A. 1951 The diffusion of heat spots in isotropic turbulence. *Proc. R. Soc. Lond.* A **209**, 418–430.